CJD and Scrapie Require Agent-Associated Nucleic Acids for Infection

Sotirios Botsios and Laura Manuelidis*

Department of Surgery, Section of Neuropathology, Yale Medical School, New Haven 06510, Connecticut

ABSTRACT

Unlike Alzheimer's and most other neurodegenerative diseases, Transmissible Spongiform Encephalopathies (TSEs) are all caused by actively replicating infectious particles of viral size and density. Different strain-specific TSE agents cause CJD, kuru, scrapie and BSE, and all behave as latent viruses that evade adaptive immune responses and can persist for years in lymphoreticular tissues. A foreign viral structure with a nucleic acid genome best explains these TSE strains and their endemic and epidemic spread in susceptible species. Nevertheless, it is widely believed that host prion protein (PrP), without any genetic material, encodes all these strains. We developed rapid infectivity assays that allowed us to reproducibly isolate infectious particles where >85% of the starting titer separated from the majority of host components, including PrP. Remarkably, digestion of all forms of PrP did not reduce brain particle titers. To ask if TSE agents, as other viruses, require nucleic acids, we exposed high titer FU-CJD and 22L scrapie particles to potent nucleases. Both agent-strains were propagated in GT1 neuronal cells to avoid interference by complex degenerative brain changes that can impede nuclease digestions. After exposure to nucleases that are active in sarkosyl, infectivity of both agents was reproducibly reduced by ≥99%. No gold-stained host proteins or any form of PrP were visibly altered by these nucleases. In contrast, co-purifying protected mitochondrial DNA and circular SPHINX DNAs were destroyed. These findings demonstrate that TSE agents require protected genetic material to infect their hosts, and should reopen investigation of essential agent nucleic acids. J. Cell. Biochem. 9999: 1–12, 2016. © 2016 Wiley Periodicals, Inc.

KEY WORDS: MICROBIOME; VIRAL STRAINS; GENOME; NEURODEGENERATION; SPHINX DNAs; PRION AMYLOID; ALZHEIMER'S DISEASE

Viruses and TSE agents are obligate intracellular parasites that depend on host-encoded susceptibility factors for their survival. In the case of TSE agents, prion protein (PrP) and other host proteins are required for productive infection [Büeler et al., 1993; Houston et al., 2015]. As with conventional viral strains, an infectious TSE agent must carry information that defines its virulence for a given host and its spread in a population. Distinct TSE agent strains have long been known to provoke large differences in incubation time and regional brain pathology in a single species. Pattison was the first to recognize that markedly different scrapie strains caused "hyper" and "drowsy" goat syndromes, and these two agents produce rapid versus slow incubation times to disease in hamsters [Pattison, 1966; Kimberlin et al., 1989]. Infectious isolates from sporadic CJD (sCJD), Asiatic CJD, New Guinea kuru, and epidemic UK BSE also show vastly different incubation times of 100–350 days in normal wt mice, and these strains provoke minimal thalamic to very widespread brain lesions [Manuelidis et al., 2009a;

Manuelidis, 2013]. The BSE agent from cows, even after replicating in humans for at least 5 years ("vCJD"), targets the same hypothalamic region in wt mice as the isolate from cows [Manuelidis et al., 2009b]. Other cross-species and epidemiologic studies also show that TSE strains are remarkably stable and the result of environmental exposure [Manuelidis, 2013; Houston et al., 2015].

The prion hypothesis insists that a normal host prion protein (PrP) spontaneously misfolds into an infectious amyloid (PrP-res) that lacks nucleic acid, yet can encode all these distinctive strains [Prusiner, 1997, 1998; Karpuj et al., 2007]. While pathological PrP-res is an excellent diagnostic marker of advanced disease, infectivity is not reduced when PrP and its PrP-res component are digested to undetectable levels by deep proteomic sequencing [Kipkorir et al., 2014]. Thus, PrP is not an essential component of the infectious particle. Moreover, Western blot PrP-res bands are tissue and cell-type specific. They are indistinguishable in wt mouse brains infected by the widely divergent kuru, CJD and scrapie agents [Manuelidis et al.,

2009a]. Conversely, lymphatic tissues produce obvious PrP-res band differences from brain but transmit the identical agent as brain homogenates. Even more dramatic PrP-res band changes occur when TSE agents are propagated in cell cultures, yet each of these agents continues to breed true and cause its original agent-specific disease, but not its PrP-res culture pattern, when inoculated back into normal mice [Arjona et al., 2004]. Individual TSE strains, like viral strains, can also block infection by a second TSE agent even when no PrP-res is produced by the protective strain [Nishida et al., 2005]. These data support a TSE viral structure with a strain-determining nucleic acid genome [Somerville, 2002; Manuelidis, 2013].

TSE agents, unlike host PrP and PrP-res, are recognized as foreign entities. This is evident from early innate immune responses of myeloid microglia to infection, but not to PrP-res or normal brain [Lu et al., 2004]. When TSE agents are transferred to cell cultures that lack inhibitory adaptive immunity, along with the many cell-type specific innate responses of brain, there is a dramatic reduction in the TSE agent doubling time from hundreds of days to 1 day [Miyazawa et al., 2011b]. Geographically restricted sources of specific TSE strains, and their containment by public health measures, also underscore the environmental origin of most TSE infections. For example, New Guinea kuru disappeared with the end of ritual cannibalization, and the epidemic UK BSE spread by trade was practically eliminated by culling infected cows. Susceptible sheep breeds also do not develop scrapie without exposure to infectious material [Houston et al., 2015]. The lack of maternal or germline transmissions in sporadic CJD (sCJD) and kuru [Gajdusek, 1977; Manuelidis and Manuelidis, 1979] further excludes a host-only agent that arises spontaneously.

Although the re-creation of infectivity from recombinant PrP in two laboratories [Legname et al., 2004; Wang et al., 2010] has received great publicity, it has not been independently reproduced with reagents proven to be agent-free [Manuelidis, 2013]. Several prion proponents acknowledge that a host "protein X" or other undefined "cofactor" is required for infection [Manuelidis, 2013], but protected nucleic acids that are present in all highly infectious preparations have been largely dismissed, as has a causal viral structure [Prusiner, 1997; Karpuj et al., 2007]. Nevertheless, chemicals that destroy conventional viral particles by releasing their nucleic acid core also release TSE particle nucleic acids and simultaneously destroy infectivity while leaving PrP/PrP-res multi-mers intact [Manuelidis et al., 2007; Botsios et al., 2015]. This structural destruction of TSE infectivity implies, but does not prove, that nucleic acids are required for TSE particle infectivity. Selective destruction of nucleic acids would.

Others have not analyzed nucleic acids in infectious preparations with any rigor, and exposure to nucleases has not previously led to a substantial loss of titer. We can find only two reports of others where infectivity was titered and a substantial amount of agent was analyzed in parallel for total nucleic acids before and after nuclease digestion. In both studies, nucleic acids were still appreciable after nuclease treatments. In the first, a P3 subcellular fraction made from 263 K scrapie hamster brain was analyzed on a 0.6% agarose gel stained with EthBr [Prusiner et al., 1980]. In accord with other's end-point determinations, the 263 K infected brain had a starting titer of 9.5 logs/gm [Kimberlin and Walker, 1977; Diringer et al., 1983] where 1 gm is equivalent to e9 cells. The P3 recovered "0–90%" of the starting infectivity along with 12% of total brain nucleic acids. These abundant nucleic acids of 3.5 to >10 kb were present before nuclease treatment in a gel loaded with only ~5 logs of P3 fractionated agent, and ≥90% of the loaded infectivity was recovered from the slot and top gel slice containing these long nucleic acids. Micrococcal nuclease digestion at the suboptimal temperature of 4°C for 16 h, followed by proteinase K (PK) in 0.2% sarkosyl for 8 h at 4°C, decreased but did not abolish P3 nucleic acids. It also did not reduce titer by >1 log (90%). The gel slot again contained most of the infectivity after nuclease-PK digestion. Subsequent DNase-Zn^2 experiments excluded analysis of long nucleic acids by using 20% acrylamide gels where silver staining revealed both nucleic acids and proteins in the phenol extracts [Meyer et al., 1991]. Higher cell equivalent (CE) loads of brain P3 showed a heavy nucleic acid smear from 200–350 nt that precluded visualization of 3e10 copies of a very faint PSTV viroid control run in a parallel control lane. These experiments failed to exclude a TSE nucleic acid genome, and also could not rule out the presence of abundant copies of a scrapie nucleic acid of viroid size.

To minimize complex neurodegenerative brain changes that might impede nuclease digestions, and to ensure that the majority of the infectious agent was being analyzed, another group digested whole homogenates of neuroblastoma cells infected with Chandler-RML scrapie agent [Neary et al., 1991]. These cells have an ~100-fold lower titer (2e7/gm) than 263 K scrapie hamster brain. Digestions done at the conventional temperature of 37°C for 4 h with a mixture of nucleases, in addition to other variations, did not reduce titer, but importantly, also left a substantial amount of nucleic acids by Schneider assay. The authors concluded that these represented a significant pool of protected nucleic acids. No viral structures or controls were added or evaluated.

Because viral genomes are protected by protein, we used Benzonase (Bz), a powerful and protease free nuclease that completely fragments all nucleic acid types, to reduce host nucleic acids. Previously, Bz digestions at 37°C for as long as 16 h without detergents did not reduce infectious particle titers from brain or cultured cells [Manuelidis, 2011]. However, protected nucleic acids of 1–16 kb were still visible on gels stained with Sybr Gold, a nucleic acid specific dye that is ~50× more sensitive than Ethidium Bromide (EthBr) [Tuma et al., 1999]. The resistant 16 kb band showed 100% sequence homology to full-length circular mitochondrial DNA (mtDNA), a bacteriophage endosymbiont relic in mammalian cells [Falkenberg et al., 2007]. In addition, two protected circular SPHINX DNAs of 1.76 kb and 2.36 kb were discovered at much lower copy numbers using a rolling circle amplification strategy. These novel sequences were present in both brain and cell culture particles. Because they were also detectable in normal preparations [Manuelidis, 2011] their role in infection is unresolved. However, antibodies to a cognate viral replication (RepA) protein (gift of D. Siddavattam, [Longkumer et al., 2013]) confirm they are transcriptionally active viral elements in both our infected and uninfected mammalian cells (unpublished observations). The identical 1.76 kb SPHINX sequence has also been independently confirmed in human material, including two Multiple Sclerosis brains [Whitley et al., 2014]. Thus PCR for mtDNA and SPHINX DNAs here provided sensitive internal viral controls for evaluating the effectiveness of nuclease digestions in parallel with the destruction of infectivity.

We used GT1 cells to find if nucleic acids were required for particle infectivity because infected GT1 cultures show no obvious cytotoxicity, produce consistent high titers, and lack complex degenerative brain changes that can impede nuclease digestions. Titers were rapidly and reliably assayed for tissue culture infectious doses (TCID), a readout that is only threefold less sensitive than expensive end-point animal assays of >300 days. This allowed us to reproducibly establish the most effective nuclease conditions. Our TCID assay is positive only for infectious particles, and is completely unresponsive to abundant PrP-res made by cells that have deleted the agent [Miyazawa et al., 2012]. In other words, this infectivity assay is unresponsive to PrP amyloid induced conversion or "seeding." This assay has been verified for diverse TSE agent-strains such as kuru, 22L scrapie and FU-CJD in both mice and murine cultures [Nishida et al., 2005; Miyazawa et al., 2011b]. Moreover, infected GT1 cells are ideal for fair comparison of agent-strains because the species and cell type are monotypic and constant. Additionally, Proteinase K (PK) and keratinase studies showed that the FU-CJD agent in GT1 cells is more sensitive to digestion than it is in diseased brain, probably a consequence of rapid agent replication in GT1 cells and/or a more open particle structure that can be more sensitive to digestion. Finally, to unmask the intrinsic properties of representative TSE agent particles, we isolated particles that contained virtually all of the starting cell titer, but had substantially reduced PrP and other host proteins [Botsios et al., 2015].

We here show reproducible and significant nuclease effects on two distinct TSE agent-strains that replicate exponentially in GT1 cells: the human FU-CJD and the sheep 22L scrapie agents. Both have high infectious titers in GT1 cells, as also verified in wt mice [Arjona et al., 2004; Nishida et al., 2005], but 22L scrapie is more sensitive than FU-CJD to chemicals that disrupt nucleic acid-protein complexes [Botsios et al., 2015]. Both agents are "solubilized" by 0.2% sarkosyl, a detergent that does not reduce titer, but that was necessary for nuclease effects. With both agent strains, ≥99% of their infectious titers are destroyed by 24 h 37°C nuclease digestions in 0.2% sarkosyl. This treatment simultaneously obliterates mtDNA and circular SPHINX DNAs, but has no effect on PrP or PrP-res.

MATERIALS AND METHODS

CELL CULTURE AND ISOLATION OF INFECTIOUS PARTICLES

Hypothalamic neuronal GT1 cells infected with either the murine adapted FU-CJD agent or the 22L scrapie agent were split at 1:4 every 4 days in parallel with uninfected controls for isolation of p18 particles as detailed [Botsios et al., 2015]. Briefly, PBS washed cells, were lysed in 1% Triton-X 100, 0.1mM PMSF, 8% sucrose in PBS at ~e8 cells/6 ml, nuclei removed by pelleting at $500g \times 5$ min, the cytosol further clarified at $10,000g \times 10$ min, and then digested for 1 h at 37°C with 120 μg/ml RNase A (10 U/mL; Calbiochem). RNase A digestion allowed rapid concentration of all infectious particles by pelleting into 20 μl of 30% sucrose at $18,000g \times 30$ min, 22°C. These p18 particles were resuspended thoroughly by bath sonication in 50 mM TrisCl 8.9 for further disaggregation [Manuelidis et al., 1995], washed with buffer and resedimented twice more. Goat anti-PrP antibody (M20, Santa Cruz Biotechnology) detected total PrP and

PrP-res on Western blots using ChemiGlow for quantitative photon signal detection [Manuelidis and Fritch, 1996]. Limited PK digestions at 25 μg/ml for 30 min gave maximal PrP-res signals, and colloidal gold staining was done after antibody detections. Table I shows the degree of particle purification from host components for the most relevant steps.

ASB14 SOLUBILIZATION AND NUCLEASE TREATMENTS

Washed p18 particles were suspended in 0.3% ASB14, incubated for 15 min at 22°C, and aliquots immediately diluted and assayed for infectivity. The ASB supernatant (sol) and insoluble (insol) particles were separated at $10,000g \times 10$ min, 22°C. The pellet was suspended in 50 mM TrisCl 8.9, spun at $14,000g \times 3$ min, and sequential supernatants pooled. Sol and insol particles were diluted to e6 CE/μl for infectivity and molecular analyses. Washed p18 particles and more purified ASB supernatants were sequentially incubated with Omni (Epicenter) and Bz (Sigma) with or without 0.2% sarkosyl and β-ME. Briefly, infectious particles from ~e7 CE were suspended by bath sonication in 50 μl of 50 mM TrisCl 8.9, 2.25 mM $MgCl_2$; 50 units of Omni was added, incubated at 37°C for 2 or 4 hr, and Bz then added for 3 or 24 hr at 37°C as detailed in Figure 2. Digestion was stopped by adding EDTA pH 8.0 to 20 mM, and aliquots diluted by >1,000 fold for infectivity assays.

INFECTIVITY TITRATIONS

Tissue culture infectious dose (TCID) were determined using standard reference end-point dilution curves for the FU-CJD and 22L-scrapie agent in mouse brain, and in GT1 cells [Liu et al., 2008; Manuelidis et al., 2009a; Miyazawa et al., 2011a, 2012]. Serially diluted particles were applied to target GT1 cells for passaging. As in animal incubations, the time for a TSE agent to induce PrP-res is dose dependent. Replicate wells of at least three different passages in the linear PrP-res readout range (≥6 Western blot determinations) showed TCID and replicate wells were indistinguishable (<10% difference). FU-CJD infected GT1 cells contain 3 TCID per cell and 22L-scrapie infected GT1 cells contain 0.03 TCID per cell (~100 fold less) in both animal and culture titrations. To avoid toxicity, final inocula concentrations were <0.002% sarkosyl, <0.002 U/μl Omni, <0.003 U/μl Bz, and <0.0006% ASB14 (ASB).

MINI NUCLEIC ACID EXTRACTIONS AND PCR

Because we found variable losses when <5e7 CE of more purified infectious particles were applied to silica columns after GdnSCN-PK digestions [Manuelidis, 2011], we developed a rapid simple protocol that quantitatively recovered nucleic acids from e6 CE particles. This allowed for immediate PCR and gel analysis. Infectious particles in 50 mM TrisCl, 20 mM EDTA pH 8.6 were first digested with 1 mg/ml PK for >4 h at 37°C to immediately destroy endogenous and added nucleases. The particle solution cleared after 10 min. Sarkosyl was added to 1% with more PK (to 2 mg/ml), and incubated 24 h before addition of PMSF to inhibit PK. This procedure destroyed PrP, other proteins and infectivity (>5 logs). An aliquot of the sample was used without further processing for gels. The same gel results were obtained when samples were EtOH precipitated or lyophilized, washed ×3 with 75% EtOH to remove salts, and then air dried before addition of 5 mM TrisCl pH 8.5 to e6 CE/μl. Alternatively, GdnSCN-

1% sarkosyl lysed particles were treated with PK as described [Manuelidis, 2011] and precipitated with acrylamide carrier. Samples were loaded in 0.2% sarkosyl-Ficoll dyes on 1.3% agarose gels and stained with Sybr gold. PCR of mtDNA was done as before [Manuelidis, 2011] using the primer pairs **MT 2.4F:** 5′CCTAGGGATAACAGCGCAA and **MT 3.3R** 5′CTAATTCTGATTCTCCTTCTG with annealing at 55°C for 20″ and extension for 1.5 min to yield a 1,003 bp fragment. The SPHINX primer pairs were also performed as previously for the 1.8 kb element (**SPX 1.8F:** 5′ CAATCATAGAAGCGAGAGAAACAGG and **SPX 1.8R:** 5′ GTTGTTCATAGCTTGCTGTGATGTC), and could be combined with the 2.4 kb element primers in one tube (**SPX 2.4F:** 5′ CACTTTGACCGTTAAGAACGGTGAAGACCTA and **SPX 2.4R:** 5′ AGTGGATAGATCGCTAAACTTAAGAGCGTA to yield the same products of 546 bp and 382 bp fragments respectively as with each primer pair alone [Manuelidis, 2011]. Annealing was for 20″ at 64°C with extension for 1 min. See accessions HQ444404.1 and HQ444405.1 for complete SPHINX sequences.

RESULTS

In contrast to nuclease experiments of others, we used optimal incubation temperatures (37°C), longer incubations of up to 24 h, a combination of the more powerful ultrapure Omnicleave (Omni) and Benzonase (Bz) nucleases, and detergents that disaggregate and solubilize more purified infectious particles. This systematic approach made it possible to conclude that the vast majority of typical infectious particles require nucleic acids for viability.

PARTICLE ISOLATION

The rapid isolation of infectious particles has been described in detail and obviates the need for sucrose gradient separations, yet achieves substantial reduction in host components using only sedimentation into a 30% sucrose cushion to separate and concentrate >85% of cell infectious p18 particles. Table I summarizes the infectious particle isolation, based on >20 independent particle preparations that included complete analysis of recovered infectivity and residual host components. As previously detailed [Botsios et al., 2015] fractionations were reproducible with small SEMs. Line A in Table I shows that 85–110% of the whole cell infectivity was recovered in the p18

washed particles. Line B shows that 70–75% of the starting protein remained in the supernatant of the 18,000 g spin (s18). Line D shows the vast majority of nucleic acids were eliminated during the initial 500 g sedimentation of nuclei from Triton X-100 lysed cells. Only 12% of the starting PrP was retained in the p18 washed pellets (line C), and no attempts were made here to remove this PrP residue before nuclease treatments. The PrP-res component of that PrP (0.3×) did not increase in isolated particles, and was not reduced by nucleases.

Both brain- and culture-derived TSE particles have the same size sedimentation and density characteristics as those previously characterized, including by field-flow fractionation, HPLC and ultrastructure [Manuelidis, 2007; Sun et al., 2008], and comparable dense virus-like particles of 20–25 nm have been demonstrated ultrastructurally in infectious particle fractions [Manuelidis, 2007] as well as in intact GT1 and N2a cells infected with different TSE agents [Manuelidis et al., 2007]. They are not present in uninfected cells. Isolated dense core particles, as those within intact cells, do not bind PrP antibodies. Because many viral particles are not always in a morphologically recognizable mature or condensed state, and detergents, can modify and/or obscure recognizable particle structure, sedimentation and infectious titer are more reliable agent properties. The zwitterionic detergent ASB14 (ASB), not previously evaluated on TSE agents, was here found to be most useful for further agent purification. Minimal sarkosyl (0.2%), that does not reduce particle titers [Botsios et al., 2015], was essential for effective nuclease digestions.

ASB14 SELECTIVELY SOLUBILIZES MOST AGENT PARTICLES

Table I summarizes multiple analyses of ASB14 on particle sedimentation. The ASB "solubilized" supernatant, shown in the rightmost row, retained 70% of the starting whole cell infectivity with even greater reduction of host proteins and nucleic acids. For graphic and numeric simplicity, the p18 washed particles are hereafter taken as 100% for Western blot and TCID assays. The M20 antibody against the central amyloid core was used to detect both the total PrP and its PrP-res component [Arjona et al., 2004; Manuelidis et al., 2009a] with different treatments. After 15 min at 22°C, ~60% of the PrP associated with FU-CJD p18 particles was solubilized by ASB. A representative blot in Figure 1A shows this solubilization (compare p18 in lane 1 and ASB sol in lane 3). The rest of the PrP was recovered in the ASB insoluble (insol) pellet (lane 5). The PrP-res component of each fraction, obtained by limited Proteinase K (PK) digestion of an aliquot for analytic purposes only are shown in the PK+ lanes loaded at 2× the CE of its parent p18, with the PrP and PrP-res amounts of each indicated at the bottom of the gel. PK was not used for any nuclease−infectivity studies because its resulting amyloid fibrils can artificially trap infectious particles. In Figure 1B colloidal gold highlights non-PrP proteins during ASB partitioning. Several ASB proteins are more prominent in the ASB pellet (insol, lane 5 dotted) than in the ASB sol (lane 3) indicating some preferential partitioning. Nucleic acid insolubility in ASB was more dramatic than for proteins and >80% of the p18 nucleic acid remained in the ASB pellet by agarose gel analysis (Table I and see below). PK digested most of the p18 particle proteins, and the strong band at 29 kd is PK (Fig. 1B, lanes 2, 4, and 6).

TABLE I. Overview of Infectivity and Molecular Components During Sequential Particle Purification

Starting total (100%)	Nuclei	s18	p18 washed	ASB-supe
A. Infectivity	5–10%	<5%	85–110%	70%
B. Protein	18–15%	70–75%	~3%	1.4%
C. %PrP /PrP-res	35%/0.3x	42%/0.25x	12%/0.3x	7.2%/0.3x
D. Nucleic acids	≥98%	nd	<0.5%	<0.1%

Summarizes the recoveries of infectivity (% starting TCID, line A) along with progressive particle purification from total host proteins (B), host prion protein (PrP) and its PrP-res component analyzed on a separate aliquot of each sample using limited PK digestion (C), and cellular nucleic acids (D). These represent titers and analyses from >20 independent preparations [Botsios et al., 2015]. The ASB data is new and detailed in the results, and the infectivity of the ASB-supe was 2.1e9/3e9 TCID.

Fig. 1. ASB14 effects on FU–CJD p18 particles. Panel A: Representative Western blot of p18 PrP (taken as 100% for subsequent treatments) and its PrP–res component (PK+ lanes) detected with the M20 antibody against the PrP amyloid core [Arjona et al., 2004; Manuelidis et al., 2009a]. Control p18 particles in lanes 1 and 2; ASB solubilized particles (sol) in lanes 3 and 4; ASB insol pellet in lanes 5 and 6. PrP in the ASB sol and insol fractions yield 100% recovery. The relative lane loads in CE (1× and 2× for PrP–res) are shown. The FU–CJD 13 kd PrP band in GT1 cells at arrow is present but faint [Nishida et al., 2005]. Panel B: Gold stained proteins of blot A. The p18 proteins (lane 1) are stronger than in the ASB fractions; the ~60 kd and 15 kd bands show incompletely stained centers typical of overloading and these contrast with the same bands in both ASB lanes 3 and 5. Several gold stained bands are much more prominent in ASB insol pellet (e.g., at dots) demonstrating differential solubilization of particular proteins by ASB. In the PK+ lanes the intense band at 29 kd is Proteinase K. Panel C graphs average PrP and its PrP–res component (lighter and darker colors respectively) in the parent p18 particles and in the ASB14 sol and insol fractions (n = 9 preparations, top graph). The FU–CJD titer per gram (e9 CE) from five independent p18 preparations (±SEM) is shown in the bottom graph. Light lavander color shows the corresponding titer of the p18 particles. The light blue bar shows that ASB solubilizes 75% of the p18 infectivity. The total p18 infectivity (3e9 TCID/gm) is recovered in the two ASB fractions. Relative lane loads are in CE.
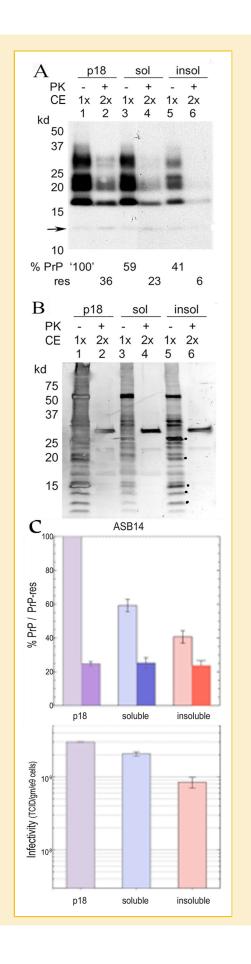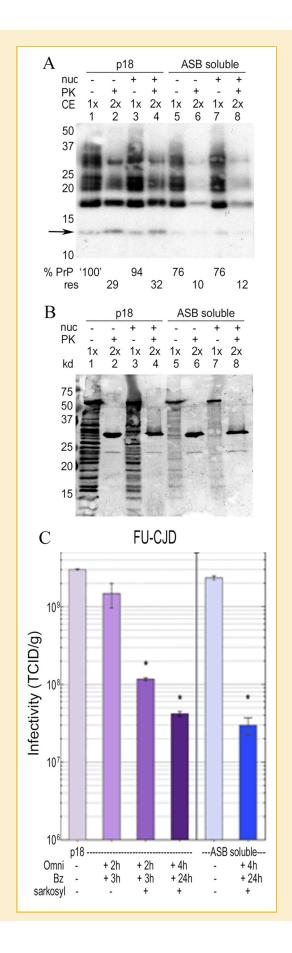
Figure 1C graphs the average (±SEM) of independent ASB fractionations (n = 9) analyzed for PrP (top), and for infectious titer (bottom). The % PrP solubilized by ASB (lavender bar) and its PrP-res component (adjacent purple bar) confirms its reproducible partitioning by ASB. We thought ASB solubilization might further disaggregate infectious particles to yield improved nuclease digestions. ASB had no detrimental effect on p18 titer, and the majority of infectious particles (~75%) were solubilized and further purified by ASB partitioning. The p18 titer is shown in the corresponding lavender bar at bottom (3e9 TCID/gm). The light blue bar shows the ASB sol component with 75% of the parent p18 infectivity, and the ASB insol pellet (pink bar) titers are shown. There was little variation in five independent p18 preparations assayed for infectivity. We therefore chose both high titer preparations, that is, the less pure p18 particles and the more purified ASB solubilized particles, to test if nucleases with and without sarkosyl induce a significant reduction in titer. A ≥1 log or ≥90% reduction is biologically as well as statistically significant. These parent p18 and ASB sol preparations contained >85% and 70%, respectively, of the starting cell titer. ASB-enhanced particle purification was not required for nuclease inactivation.

NUCLEASE EFFECTS ON P18 AND ASB SOL PARTICLES IN FU-CJD

We first evaluated nuclease effects on host proteins in control untreated p18 particles and after exposure to nucleases. As shown in Figure 2A, even after maximal nuclease digestions conditions (24 h Omni + Bz in 0.2% sarkosyl) no band changes were detectable in PrP in the p18 without (lane 1) and with (lane 3) nucleases (+nuc lanes). The amount of PrP was not significantly reduced with nucleases (94% of the p18) and the PrP-res component (lanes 2 and 4) showed slightly more PrP-res in the nuc+ aliquot (32% vs. 29% in the control). Such small differences are within aliquot variation. The ASB sol fraction also showed no PrP changes with nucleases (compare lanes 5 and 7) in band pattern or amount. Both had 76% of the p18 PrP. Again, the PrP-res component in both ASB fractions was comparable (10–12%). Gold binding proteins on this same blot
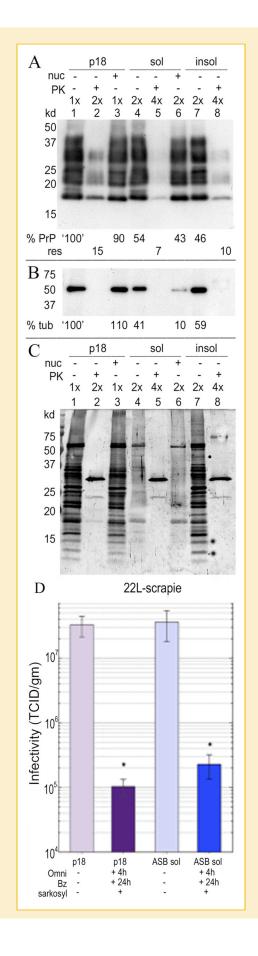
Fig. 2. Control and nuclease digested parent p18 and ASB solubilized FU–CJD particles. The PrP–res in PK+ lanes is analytical only since no titers were done on PK digested material. Panel A: Representative Western blot. The p18 PrP, and its PrP–res component (at 2× CE loads) does not change after 24 h of nuclease digestion in sarkosyl (compare control lanes 1 and 2 with nuc+ lanes 3 and 4). ASB solubilized 76% of the p18 PrP (sol lanes). Again, PrP and its PrP–res component are not altered by nucleases (compare lanes 5 and 6 with 7 and 8). Independent preparations (n > 6) showed the same PrP/PrP–res profiles. Panel B: Gold stained proteins on the same blot also revealed no changes in the many visualized p18 proteins after 24 h digestion with nucleases + sarkosyl (lanes 1 and 3). Similarly, no change with nuc+ was seen in the ASB sol proteins with substantially lower protein levels than the p18. Panel C: FU–CJD infectivity (TCID per gm, ± SEM) from three independent p18 preparations treated as indicated; The recovered 3e9 TCID/gm in the p18 (lightest lavender bar) is the same as in Figure 1 and multiple previous experiments [Miyazawa et al., 2011a; Botsios et al., 2015]. Short nuclease treatment without sarkosyl (adjacent darker bar, 2 h Omni + 3 h Bz) shows no significant titer decrease ($P = 0.08$). The same short incubation conditions with sarkosyl significantly decreases titer by 97% (third darker bar, $^*P < 0.001$). After 24 h, a two log (99%, $P < 0.0001$) titer loss is seen (darkest purple bar). ASB sol particles (light blue bars) without nucleases in right panel also show no significant titer decrease from the parent p18, and 99% of the infectivity is again destroyed by 24 h nuclease treatment with sarkosyl. In sum, infectivity is significantly reduced by nucleases (99%) in both the total p18 and the ASB sol fraction while PrP and gold binding proteins remain unchanged. Anova and t-tests both yielded the same P values.

further confirmed a more general lack of protein changes with maximal nuclease conditions, as shown in Figure 2B. The p18 control (lane 1) and nuc+ (lane 3) particles are virtually identical. Similarly, the ASB solubilized particles with much less protein than the p18, also showed no clear differences in gold stained proteins. Greater agent purification of the ASB sol particles is evident by the vast reduction in their gold stained proteins as compared to those in the parent p18 (lanes 5 and 7 vs. 1 and 3, respectively). PK treated aliquots for these gold-stained proteins were not informative.

Previous studies showed 0.2% sarkosyl was sufficient to solubilize all p18 particles with no titer loss [Botsios et al., 2015]. Thus, we compared the efficacy of 3 h Omni + 2 h Bz with and without sarkosyl for infectivity (TCID) titrations. Without sarkosyl, no significant reduction in FU-CJD titer was seen as compared to the untreated p18 controls (Fig. 2C, lavender and next darker bars). Long DNA sequences, including protected 16 kb mtDNA also remained intact, in accord with previous observations [Manuelidis, 2011]. We then evaluated the effect of sarkosyl, and found significant progressive losses of titer with nuclease incubation times. Because detergent micelles can prevent or retard penetration of added components, we added Omni for 2–4 h, and then added sarkosyl plus Bz for an additional 3 or 24 h. This strategy could enhance Gibbs–Donnan molecular exchanges between the inner and outer micelle compartments to yield increasingly complete digestions. In contrast to the no sarkosyl 5 h controls, 97% (1.1e8/3e9 TCID, $P < 0.001$) of the FU-CJD p18 infectivity was destroyed in the presence of sarkosyl (Fig. 2C, third darkest bar). After 24 h, 99% of agent particles were inactivated (darkest bar). This graph also shows the more purified ASB sol fraction before (light blue) and after 24 h nuclease digestions with sarkosyl (dark blue bar) in the right most panel. Again 99% of the FU-CJD agent is destroyed by nucleases even though its PrP and PrP-res component is preserved. In sum, only 1% of FU-CJD particles remain viable after 24 h nuclease-sarkosyl treatment. Since 85–

Fig. 3. p18 and ASB14 solubilized 22L–scrapie particles. Panels A–C show PrP and protein solubilization, and D shows the corresponding TCID/gm before and after nuclease treatment. Nuclease destroys 99.7% (2.52 logs) of the 22L scrapie agent. A: Representative scrapie blot of PrP in the p18 and the ASB sol fraction before and after 24 h nuclease + sarkosyl treatment (nuc + lanes). Lane 1 shows the PrP of p18 particles without nucleases and after 24 h nucleases (lane 3); the PrP in both is indistinguishable. ASB sol particles without and with nucleases are also unchanged as shown in lanes 4 and 6, respectively. The PrP–res component of the p18 and ASB sol and insol fractions is shown at bottom of each PK+ lane. B: Tubulin shows equal loads (−PK lanes) and is completely digested by PK (+lanes 2, 5, 8). Reduction of tubulin is seen only in nuclease treated ASB sol particles with nucleases plus Ca++. C: Gold stained proteins on the same blot and in contrast to Figure 2, increased lane loads (2× and 4×) were used for ASB subfractions for better visualization of the reduced proteins. The ASB solubilizes selective proteins with preferential pelleting of several proteins (lane 7, as at dots). PrP–res of gold stained proteins, as shown, was uninformative. D: Infectivity (TCID) per gram (e9 cell equivalents) of 22L–scrapie particles where control p18 particles (lavender bar) have 3e7 TCID/gm, as in previous preparations [Liu et al., 2008]. Incubations of parallel aliquots without nucleases showed no titer loss, in contrast to a ≥2.5 log loss by nucleases in both the p18 (purple bar) and ASB sol particles (dark blue bar).

110% of the starting whole cell infectivity is recovered in the p18, the vast majority of the FU-CJD agent population requires particle-associated nucleic acid.

22L SCRAPIE PARTICLES HAVE ENHANCED NUCLEASE SENSITIVITY

Various TSE agent-strains display different susceptibilities to inactivation, and FU-CJD and 22L scrapie particles from GT1 cells show intrinsic chemical resistance differences [Botsios et al., 2015]. To test if 22L scrapie particles are more sensitive to nuclease inactivation than FU-CJD particles both the p18 and ASB sol scrapie particles were exposed to the same 24 h nuclease digestion as above. Because 22L scrapie has an almost two log lower titer (∼3.3e7 TCID/gm) than FU-CJD particles from GT1 cells, the scrapie particles will have a higher ratio of non-specific host sequences to agent. Thus, they might be less susceptible to destruction by nucleases. This was not the case.

Figure 3A–C shows the p18 and its derivative ASB sol and insol particles in a representative blot stained for PrP/PrP-res, tubulin and gold binding proteins. The pattern of progressive purification of 22L infectious particles was the same as with FU-CJD (included in the Table I summary). Again, the PrP pattern was not affected by 24 h nuclease digestions in 0.2% sarkosyl, as shown in control lane 1 and in the nuc+ lane 3, and minor differences in amount are within the range of experimental variation. The ASB sol and insol PrP (lanes 4 and 7) recover 100% of the p18 PrP. In 22L scrapie, nuclease digestion again failed to detectably alter the PrP band pattern in the ASB sol fraction (compare lanes 4 and 6). As with FU-CJD, the PrP-res component was reduced in the 22L scrapie ASB sol fraction as compared to the parent p18 fraction (lane 2 versus lane 5). Tubulin detection in the same blot is shown in panel B. It demonstrates there is no nuclease effect on tubulin in the p18 after nuclease incubation (lanes 1 and 3), and tubulin partitions almost equally in the ASB sol and the ASB insol pellet (41% vs. 59%, lanes 4 and 7 in blot B). Tubulin in multiple experiments was always completely digested by PK (as in lanes 2, 5, and 8). Interestingly, tubulin was variably reduced in the Ca++ nuclease treated ASB sol fraction as compared

to its constant state in the p18. Lane 6 shows the most extreme example of this reduction in our studies (compare ASB sol lanes 4 and 6). Because both Omni and Bz are genetically engineered, chromatographically purified, and showed no proteolytic activity in manufacturer's tests or ours, it is likely that the breakdown of tubulin exclusively in the ASB sol fraction is related to the long incubation with Ca++ ions known to destabilize tubulin complexes. The ASB control did not contain Ca++. Panel C further shows that all detectable gold stained proteins were again faithfully preserved in the nuclease treated p18 (compare lanes 1 and 3). In this gel, we loaded $2\times$ the amount of the ASB sol fraction (rather than the $1\times$ CE in Fig. 2) to increase the visualization of reduced gold protein in the ASB sol fraction, and no change was observed after nuclease digestion (compare lanes 4 and 6). In sum, nucleases showed no detectable effect on any protein except non-infectious tubulin in the ASB sol fraction.

Despite the higher host to agent ratio in 22L scrapie, nuclease reduced titer more than in FU-CJD. Panel D graphs the TCID/gm.

There is a 99.7% titer decrease in the p18 (lavender versus purple bar), equivalent to a 2.52 log or 330-fold decrease ($P < 0.0001$), that is, only 1 of 330 scrapie particles remains viable after nuclease digestion. The more purified ASB sol scrapie particles show a comparable loss of 99.5% (dark blue bar), and the reduced tubulin in this fraction induced no additional loss of titer. In sum, isolated 22L scrapie agent particles appear to be more sensitive than FU-CJD particles to nuclease digestion.

DESTRUCTION OF PROTECTED DNAS IN VIRAL STRUCTURES COINCIDE WITH THE LOSS OF AGENT TITER

For nucleic acid analysis, a rapid PK stripping procedure was developed that was reproducible and could be used directly for both gel analysis and subsequent PCR tests. Nucleases without sarkosyl did not compromise extraction of long nucleic acids previously (see Methods and Manuelidis [2011]) and nucleic acids extracted from titered particles before and after nuclease are representatively shown in Figure 4. These 1.3% agarose gels show ASB partitioning of
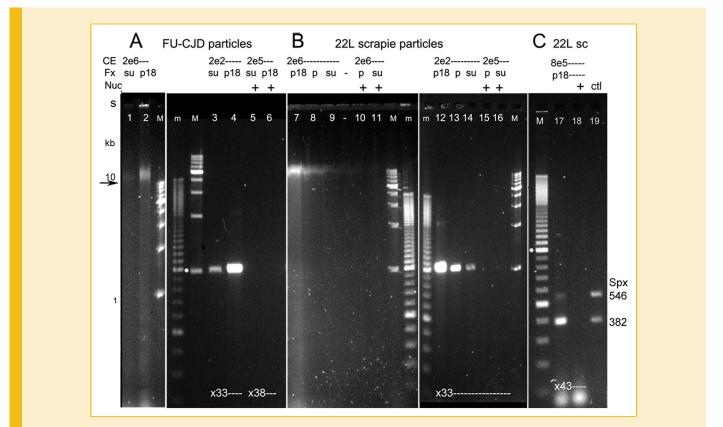

Fig. 4. Nucleic acid analyses of p18 and ASB particle fractions in FU–CJD (panel A) and in 22L scrapie (panels B and C). Parent p18 nucleic acids in A shows only a small amount of FU–CJD nucleic acids remain in the ASB soluble particles (compare su in lane 1 and p18 in lane 2). The su shows only a faint 16 kb band (above 10 kb arrow) as compared to the much stronger p18 nucleic acids of ∼16 kb. Similarly, the solubilized ASB su in 22L scrapie (B, lane 9) contains barely detectable nucleic acids in comparison with its parent p18 (lane 7) and the counterpart residual insol ASB pellet (p, lane 8). Nuclease treated ASB pellets (lane 10, +) and ASB solubilized particles (lane 11, +) show no detectable nucleic acids. Corresponding PCR for mtDNA of each sample before and after 24 h nuclease treatment are shown in lanes 3–6 for FU–CJD, and lanes 12–16 for 22L scrapie. There are strong mtDNA 1 kb PCR bands in the non–nuclease treated samples (lanes 3, 4, 12–14) that correspond in intensity to the relative DNA content of each particle fraction. In contrast, DNA is absent in nuclease treated FU–CJD particles (lanes 5, 6, 10, and 11) with indicated cycles and CE inputs that are 1,000 fold greater than in the non–nuclease samples. Panel C shows the PCR with a high CE input for combined SPHINX 1.76 (at 546 bp) and for SPHINX 2.36 (382 bp) as previously described [Manuelidis, 2011], and both bands are present (lane 17). The less purified p18 required 4,000 greater input for positive SPHINX signals than mtDNA using the same preparations as shown in B, in addition to 10 additional PCR cycles. Neither band was detectable by PCR after 24 h nuclease treatment of particles (lane 18). Lane 19 shows a control PCR of both SPHINX elements with ∼5 ng/band. The 100 bp marker (m) and the 1–10 kb ladder (M) lanes are indicated, and each band in the 1 kb ladder contains 3 ng DNA except for the 5 kb band which contains 9 ng. With Sybr gold staining, a pure 1 kb ds band without background would require ≥600 pg, with more needed to visualize a 2 kb ss RNA.

nucleic acid complexes for FU-CJD and 22L scrapie particles, with PCR for protected DNAs before and after 24 h nuclease-sarkosyl. Panel A shows the FU-CJD ASB sol nucleic acids (lane 1, su) compared to the parent p18 particle nucleic acid at the same load on each lane (2e6 CE). There are visible long nucleic acids at ~16 kb the p18 (lane 2 just above the arrow at 10 kb marker band), and a much fainter smear of other heterogeneous nucleic acids in the gel. Nucleic acids are visibly reduced in the ASB sol (su), and the 16 kb band is also tighter, indicating less nuclear DNA contamination (lane 1). Aliquots treated with DNase I, as previously [Manuelidis, 2011], abolished these naked nucleic acids. No FU-CJD band was visualized in comparison to parallel noninfectious preparations, nor would they be expected. Unlike lytic and highly productive viruses, FU-CJD has a maximal TCID of three infectious particles per cell, that is, ~5e6 infectious particle nucleic acids loaded on these lanes. At this level, a 1 kb DNA or 2 kb RNA has 9.1e5 copies of agent nucleic acid per pg, that is, maximally 6 pg in this gel. This is well below our detection levels if the TSE agent, like poliovirus, has a 1:1 particle nucleic acid to titer ratio. Even 10 nucleic acids per infectious agent particle would be undetectable (60 pg). Given the intensity of the 3 ng per band in the 1 kb marker (M lanes), >600 pg of agent nucleic acid (equivalent to a gel load of ~2e8 CE or 6e8 TCID) would be needed to detect a TSE-specific band. Indeed, this was the reason for originally using a rolling circle amplification strategy to discover novel sequences, such as SPHINX DNAs, in particle preparations [Manuelidis, 2011].

The solubilized ASB su in Figure 4A (lane 1) shows ~1/10th the nucleic acid of its parent p18 particles (lane 2) at the same CE load. This demonstrates a high degree of nucleic acid purification in this fraction with respect to starting cell nucleic acids. Since GT1 cells contain ~30 pg/cell of nucleic acid (RNA + DNA), ASB sol particles contain <0.002% of starting whole cell nucleic acids (2e6 CE particles with ≤1 ng vs. 6e4 ng in 2e6 cells). PCR for mtDNA in this ASB su and in the parent p18 further shows that before 24 h nuclease treatment only 200 CE input yields a very strong 1 kb mtDNA PCR band after 33 cycles whereas the ASB sol yields a much fainter band that reflects its reduced nucleic acid (compare lanes 3 and 4). In contrast to these strong PCR products, nuclease treated FU-CJD particles with a 1,000-fold greater input (2e5 CE), and 38 amplification cycles, show no mtDNA band (lanes 5 and 6). Thus 24 h nuclease-sarkosyl digestions abolished the compact protected mtDNA in both p18 and ASB sol nuclease samples. This demonstrates that the FU-CJD titer losses depended on nucleic acid destruction.

Panel B shows 22L scrapie particles with the p18, ASB insol (p), and ASB sol (su) in lanes 7, 8, 9, respectively. The control p18 again contains a strong band at 16 kb with some heterogeneous nucleic acids from 10 kb to 50 nt. The insol pellet selectively retains most of these molecules (lane 8, p) while the more purified infectious ASB sol (lane 9, su) retains <0.005% of whole cell nucleic acids. The ASB pellet and ASB sol particles treated with nucleases (lanes 10 and 11) show no visible nucleic acids at the same CE load. The corresponding PCR panel again confirms the increased purification in control ASB sol particles at an input of only 200 CE where most of the amplified mtDNA remains in the less infectious ASB pellet versus the ASB soluble su (lanes 13 and 14). The parallel aliquot of these samples after nuclease treatment again produced no mtDNA band after 33 cycles even with a 1,000 fold higher input of 2e5 CE.

Panel C further shows that two circular viral SPHINX sequences were also destroyed by nucleases. These DNAs were previously identified as resistant to nuclease digestions without sarkosyl and they are present at much lower copy numbers in particle fractions than mtDNA. As shown in lane 17, they required a 4,000 fold input of 8e5 CE with 43 PCR cycles using the less purified p18. The upper 546 bp band is from SPHINX 1.76 and the 382 bp band is from the 2.36 SPHINX element. In this p18 sample, the 2.36 element is dominant. With nucleases (lane 18) no signal was detected for either SPHINX element. Both 22L scrapie samples are from preparations assayed above for infectivity, and a control DNA shows a PCR of both bands (lane 19) from material in the original report where equal amounts of each element were found in infectious sucrose fractions from hamster brain. The higher infectivity FU-CJD p18 sample without nuclease contained more intense SPHINX elements, and had a stronger 1.76 band. Nuclease digestion that abolished infectivity also abolished both SPHINX elements (data not shown). In sum, it is clear that nucleases also destroy both SPHINX genomes along with infectivity while leaving PrP and other proteins undiminished.

Figure 5 shows representative cell assays used to determine tissue culture infectious doses (TCID) in experiments here with FU-CJD and 22L scrapie particles. In these assays, duplicate wells of indicator GT1 cells are exposed to equal cell equivalents (1× CE) of uninfected (mock lanes) and infectious particles. Uninfected cells, including those with high PrP-res that have deleted the infectious agent [Miyazawa et al., 2012], do not induce a PrP-res response when applied to indicator cells. In contrast, infected brain and cultures provoke a PrP-res response. A lower infectious dose takes a longer time, with additional passages, to elicit PrP-res. Panel A in Figure 5 shows uninfected material (mock) elicits no PrP-res (PK+ lane 2) even at 8× the CE loaded on the gel along with 1× of its undigested PrP (lane 1). As shown, the p18 (100% reference TCID) provokes more PrP-res than the ASB sol and insoluble fractions. Their TCID represent 75% and 25% of the p18 particle titer. Panel B shows a 12× load of the mock sample elicits no PrP-res (PK+ lane 2) while the PrP-res in the 22L scrapie sample (lanes 4 and 6) shows a strong PrP-res response. After nuclease digestion of these p18 particles almost no PrP-res is induced (lanes 8 and 10) during the same cell passage. This demonstrates substantial loss of infectivity equivalent to <1% of the parent p18 TCID. The ASB sol control and nuclease treated particles also show a comparable loss of titer (lanes 12 and 14, respectively).

DISCUSSION

We previously showed that isolated brain particles without detectable PrP maintain their high infectivity, a finding that excludes a prion protein agent [Kipkorir et al., 2015]. The above results demonstrate that particles from two different agent strains require protected nucleic acids for infection. PrP and its PrP-res component were not affected by nuclease digestion, yet after nucleases these proteins yielded no significant infectivity, a finding
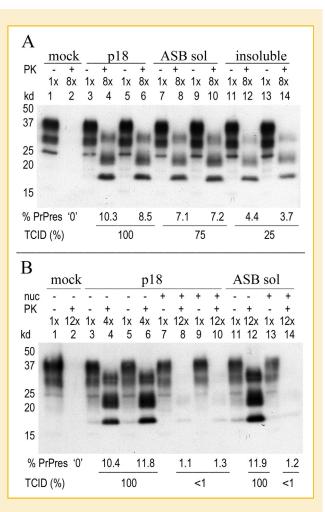
Fig. 5. Representative Western blot of titrations for FU–CJD and 22L–scrapie for determining tissue culture infectious doses (TCID). Assays were done as previously, for example, Liu et al., [2008]. Panel A: Duplicate wells of indicator GT1 cells are exposed to equal cell equivalents (1× CE) of uninfected (mock lanes) and FU–CJD p18 particles. The p18, ASB sol and ASB insol lanes contain the same 1× CE. PrP-res is shown in the PK+ lanes at 8× CE. Uninfected mock material elicits no PrP-res (lane 2, PK+). In contrast, the infected FU–CJD p18 particles provoke strong PrP-res bands (PK+ lanes 4 and 6 from duplicate wells). The ASB sol samples (lanes 8 and 10) also show a strong PrP-res response, equivalent to 75% of the total p18 TCID whereas the ASB insol particles (lanes 12 and 14) show less PrP-res, equivalent to 25% of the p18 TCID, that is, all the starting p18 TCID are recovered after ASB partitioning. Panel B: Untreated 22L–scrapie p18 particles, and the nuclease treated p18 and ASB sol particles (nuc+ lanes) show marked reduction in infectivity after nucleases. Mock control again shows no PrP-res (lane 2, even at 12× CE load) whereas p18 scrapie and ASB sol particles provoke a strong PrP-res response (lanes 4, 6, and 12). Nuclease exposure for 24 h of both the p18 and ASB sol particles markedly reduces infectivity as shown by minimal PrP-res, even at 12× CE loads (lanes 8, 10, and 14). This low level of PrP-res is equivalent to <1% of the p18 control TCID. Later cell passages showed a low PrP-res signal in the linear range, which allowed a more accurate titer quantitation (as graphed in Fig. 3D). This assay can assess a six log loss [Botsios et al., 2015]. Markers in kd.

that further questions the reality of the infectious PrP hypothesis. A causal virus that can encode unique agent strains, and is environmentally derived, is the most plausible TSE agent structure. These findings have fundamental ramifications, and open new avenues for the discovery, prevention, and treatment of chronic diseases of unknown cause. In the realm of late-onset neurodegenerative diseases, it is possible that a subset of Alzheimer's disease is initially set in motion by unrecognized environmental pathogens of low virulence that are no longer actively replicating at later stages of neurodegeneration.

The above data demonstrates yet again that isolated TSE infectious particles, characterized by their homogeneous size, and density separation into 30% sucrose, contain many protected nucleic acids of viral size. Nucleases destroyed all visible nucleic acids along with infectivity. Improved particle isolation procedures that recovered 85–100% of the starting infectivity along with rapid and quantitative culture assays for infectivity, rather than PrP-res amyloid seeding, revealed unambiguous titer losses of >99% after straightforward nuclease digestion. These data provide compelling arguments for reinvigorating experiments to identify causal agent nucleic acids in TSE (PrP amyloid) diseases. In contrast to previous limited nuclease studies, the positive demonstrations of TSE agent destruction here is based, at least in part, on particle isolation procedures that minimized PrP and many extraneous host proteins, reduced background nucleic acids to very low levels (<0.01% of whole cells), used extended incubations with more powerful nucleases at 37°C, and included sarkosyl in buffer conditions that disaggregate PrP amyloid but do not affect infectivity.

PCR for mtDNA, an endogenous virus-like structure, also provided a superior quantitative assay for complete digestion of protein-protected nucleic acids. Nucleases in others' previous studies failed to destroy obvious nucleic acids and hence no significant titer decrease was observed. Those nuclease experiments may also have been compromised by the typically small (0.5–5%) agent population investigated which selectively copurified with amyloid [Manuelidis, 2013]. PrP amyloid and associated plaque molecules in brain can trap the infectious agent with other molecules in an insoluble and poorly permeable aggregate [Manuelidis et al., 1997] that hinders effective nuclease digestions, and PrP-res accumulation is an innate host response that can help to clear infection [Miyazawa et al., 2012]. The tiny population of agent that remained viable in our nuclease studies could similarly reside in a resistant PrP aggregate, or in a keratinase resistant protein or biofilm [Miyazawa et al., 2011a; Botsios et al., 2015].

The requirement for agent nucleic acids was demonstrated with two very different TSE strains, and 22L scrapie agent particles were more susceptible to nuclease inactivation than FU–CJD. This difference parallels the greater sensitivity of 22L scrapie to chemical disruption, and emphasizes molecular or structural differences among agent strains that cannot be ascribed to host species or cell type. The invariant phenotype of individual TSE agent strains despite passage in different species and cell types suggests a DNA rather than a typical single stranded RNA viral genome. While we do not know if particle RNA, DNA, or both are required for infection, it is now possible to resolve these alternatives using advanced deep sequencing methods to probe nucleic acids in the more purified highly infectious ASB sol particles.

The concept that a TSE virus induces a pathological PrP-res amyloid change is not unlike recent observations made for other viral infections. TSE agents all replicate exponentially, and only later

induce PrP-res amyloid in an arithmetic process that barely increases the total PrP [Manuelidis, 2013]. Other viruses also induce protein aggregates that are "prion-like" and antiviral [Hou et al., 2011]. Mammalian viruses can also initiate changes that lead to protein aggregation and pathology years after infection, as in post-encephalitic Parkinson's disease. Subacute paramyxovirus infections also induce neurofibrillary tangles that are indistinguishable from those commonly found in standard non-infectious Alzheimer's disease (AD) brain, as well as in brains subjected to repeated trauma (dementia pugilistica). Many of these protein aggregates can transfer between cells in a non-infectious process. Hence, it is misleading to equate such pathological protein transfers with an active and real infectious process in mammals. Despite recent claims, AD amyloid is not infectious. It cannot be serially passaged or diluted, and it only accelerates old age neuropathologic changes when massive amounts are injected intracerebrally into aging primates [Ridley et al., 2006; Manuelidis, 2013]. While protein misfolding and amyloid seeding can occur in both artificial test tube and in vivo settings, and pathologic overlaps between TSEs and other neurodegenerative diseases such as AD have been highlighted for years, the term prion has become all-inclusive. It obscures differences among these diseases that have heterogeneous and largely unknown origins.

Interestingly, Herpes simplex virus can also initiate β-amyloid processes [Civitelli et al., 2015] and other environmental viruses may incite, contribute to and/or define different AD subsets. We identified two environmental viral metagenomic sequences hidden in TSE particle nucleic acids, and these were in the expected low amounts for TSE agent titers [Manuelidis, 2011]. Because these circular SPHINX DNAs (acronym for Slow Progressive Hidden INfections of variable X latency) can also be found in uninfected cells and brain, their DNA presence is insufficient to be the sole cause of TSE infection. It remains to be seen if their transcriptional activity, or antibody detected Rep A or other ORF proteins give them different attributes. SPHINX DNAs were not detectable in our reagents in numerous tests, indicating they were not lab contaminants, and the 1.76 element was identified in two human Multiple Sclerosis brains and sera in Germany [Whitley et al., 2014]. This further independently links them to progressive brain pathology. The circular structure of these elements is also consistent with a satellite type of virus, one that may need additional molecular components for infection. This circular DNA structure also led us to suggest they might have a role in neoplastic transformation [Manuelidis, 2011]. Interestingly, because of their presence in many cows, combined with the epidemiology of milk and meat consumption and breast cancer, zur Hausen [2015] recently proposed they have a role in breast tumors. A more widespread source for these remnant phage DNAS of commensal Acinetobacter may also be considered because as previously shown, brains from laboratory hamsters and mice contained both SPHINX sequences even thought these rodents have no known exposure to cow's milk. The finding of these DNAs in TSE infectious particles surely should encourage a deeper investigation of viral nucleic acids in TSEs, and probably other neurodegenerative diseases. Because these small circular sequences were present in brain tissue without any accompanying Acinetobacter sequences, it suggests they can replicate symbiotically in mammalian cells. It remains to be seen if they have been incorporated during mammalian evolution or after birth. Regardless, they may represent the tip of the iceberg of other unsuspected bacterial viruses that can be incorporated by mammals and sometimes act as stealth pathogens.

REFERENCES

Arjona A, Simarro L, Islinger F, Nishida N, Manuelidis L. 2004. Two Creutzfeldt–Jakob disease agents reproduce prion protein-independent identities in cell cultures. Proc Natl Acad Sci USA 101:8768–8773.

Botsios S, Tittman S, Manuelidis L. 2015. Rapid chemical decontamination of infectious CJD and scrapie particles parallels treatments known to disrupt microbes and biofilms. Virulence 6:787–801.

Büeler H, Aguzzi A, Sailer A, Greiner RA, Autenried P, Auget M, Weissmann C. 1993. Mice devoid of PrP are resistant to scrapie. Cell 73:1339–1347.

Civitelli L, Marcocci ME, Celestino I, Piacentini R, Garaci E, Grassi C, De Chiara G, Palamara AT. 2015. Herpes simplex virus type 1 infection in neurons leads to production and nuclear localization of APP intracellular domain (AICD): Implications for Alzheimer's disease pathogenesis. J Neurovirol 21:480–490.

Diringer H, Hilmert H, Simon D, Werner E, Ehlers B. 1983. Towards purification of the scrapie agent. Eur J Biochem 134:555–560.

Falkenberg M, Larsson NG, Gustafsson CM. 2007. DNA replication and transcription in mammalian mitochondria. Annu Rev Biochem 76:679–699.

Gajdusek DC. 1977. Unconventional viruses and the origin and disappearance of kuru. Science 197:943–960.

Hou F, Sun L, Zheng H, Skaug B, Jiang QX, Chen ZJ. 2011. MAVS forms functional prion-like aggregates to activate and propagate antiviral innate immune response. Cell 146:448–461.

Houston F, Goldmann W, Foster J, Gonzalez L, Jeffrey M, Hunter N. 2015. Comparative susceptibility of sheep of different origins, breeds and PRNP genotypes to challenge with bovine spongiform encephalopathy and scrapie. PLoS ONE 10:e0143251.

Karpuj MV, Giles K, Gelibter-Niv S, Scott MR, Lingappa VR, Szoka FC, Peretz D, Denetclaw W, Prusiner SB. 2007. Phosphorothioate oligonucleotides reduce PrP levels and prion infectivity in cultured cells. Mol Med 13:190–198.

Kimberlin RH, Walker C. 1977. Characteristics of a short incubation model of scrapie in the golden hamster. J Gen Virol 34:295–304.

Kimberlin RH, Walker CA, Fraser H. 1989. The genomic identity of different strains of mouse scrapie is expressed in hamsters and preserved on reisolation in mice. J Gen Virol 70:2017–2025.

Kipkorir T, Tittman S, Botsios S, Manuelidis L. 2014. Highly infectious CJD particles lack prion protein but contain many viral-linked peptides by LC-MS/MS. J Cell Biochem 115:2012–2021.

Kipkorir T, Colangelo CM, Manuelidis L. 2015. Proteomic analysis of host brain components that bind to infectious particles in Creutzfeldt–Jakob disease. Proteomics 17:2983–2998.

Legname G, Baskakov I, Nguyen H, Riesner D, Cohen F, DeArmond S, Prusiner S. 2004. Synthetic mammalian prions. Science 305:673–676.

Liu Y, Sun R, Chakrabarty T, Manuelidis L. 2008. A rapid accurate culture assay for infectivity in transmissible encephalopathies. J Neurovirol 14:352–361.

Longkumer T, Kamireddy S, Muthyala VR, Akbarpasha S, Pitchika GK, Kodetham G, Ayaluru M, Siddavattam D. 2013. Acinetobacter phage genome is similar to Sphinx 2.36, the circular DNA copurified with TSE infected particles. Sci Rep 3:2240.

Lu ZH, Baker C, Manuelidis L. 2004. New molecular markers of early and progressive CJD brain infection. J Cellular Biochem 93:644–652.

Manuelidis EE, Manuelidis L. 1979. Experiments on maternal transmission of Creutzfeldt–Jakob disease in guinea pigs. Proc Soc Exp Biol Med 160:233–236.

Manuelidis L, Fritch W. 1996. Infectivity and host responses in Creutzfeldt–Jakob disease. Virology 216:46–59.

Manuelidis L. 2007. A 25 nm virion is the likely cause of transmissible spongiform encephalopathies. J Cell Biochem 100:897–915.

Manuelidis L. 2011. Nuclease resistant circular DNAs copurify with infectivity in scrapie and CJD. J Neurovirol 17:131–145.

Manuelidis L. 2013. Infectious particles, stress, and induced prion amyloids: A unifying perspective. Virulence 4:373–383.

Manuelidis L, Sklaviadis T, Akowitz A, Fritch W. 1995. Viral particles are required for infection in neurodegenerative Creutzfeldt–Jakob disease. Proc Natl Acad Sci USA 92:5124–5128.

Manuelidis L, Fritch W, Xi YG. 1997. Evolution of a strain of CJD that induces BSE-like plaques. Science 277:94–98.

Manuelidis L, Yu ZX, Barquero N, Mullins B. 2007. Cells infected with scrapie and Creutzfeldt–Jakob disease agents produce intracellular 25 nm virus-like particles. Proc Natl Acad Sci USA 104:1965–1970.

Manuelidis L, Chakrabarty T, Miyazawa K, Nduom NA, Emmerling K. 2009a. The kuru infectious agent is a unique geographic isolate distinct from Creutzfeldt–Jakob disease and scrapie agents. Proc Natl Acad Sci USA 106:13529–13534.

Manuelidis L, Liu Y, Mullins B. 2009b. Strain-specific viral properties of variant Creutzfeldt–Jakob disease (vCJD) are encoded by the agent and not by host prion protein. J Cell Biochem 106:220–231.

Meyer N, Rosenbaum V, Schmidt B, Gilles K, Mirenda C, Groth D, Prusiner SB, Riesner D. 1991. Search for a putative scrapie genome in purified prion fractions reveals a paucity of nucleic acids. J Gen Virol 72(Pt1):37–49.

Miyazawa K, Emmerling K, Manuelidis L. 2011a. High CJD infectivity remains after prion protein is destroyed. J Cell Biochem 112:3630–3637.

Miyazawa K, Emmerling K, Manuelidis L. 2011b. Replication and spread of CJD, kuru and scrapie agents in vivo and in cell culture. Virulence 2:188–199.

Miyazawa K, Kipkorir T, Tittman S, Manuelidis L. 2012. Continuous production of prions after infectious particles are eliminated: Implications for Alzheimer's disease. PLoS ONE 7:e35471.

Neary K, Caughey B, Ernst D, Race RE, Chesebro B. 1991. Protease sensitivity and nuclease resistance of the scrapie agent propagated in vitro in neuroblastoma cells. J Virol 65:1031–1034.

Nishida N, Katamine S, Manuelidis L. 2005. Reciprocal interference between specific CJD and scrapie agents in neural cell cultures. Science 310:493–496.

Pattison I. 1966. The relative susceptibility of sheep, goats, and mice to two types of the goat scrapie agent. Res Vet Sci 7:207–212.

Prusiner SB. 1997. Prion disease and the BSE crisis. Science 278:245–251.

Prusiner S. 1998. Prions. Proc Natl Acad Sci USA 95:13363–13383.

Prusiner SB, Groth DF, Bildstein C, Masiarz FR, McKinley MP, Cochran SP. 1980. Electrophoretic properties of the scrapie agent in agarose gels. Proc Natl Acad Sci USA 77:2984–2988.

Ridley RM, Baker HF, Windle CP, Cummings RM. 2006. Very long term studies of the seeding of beta-amyloidosis in primates. J Neural Transm 113:1243–1251.

Somerville RA. 2002. TSE agent strains and PrP: Reconciling structure and function. Trends Biochem Sci 27:606–612.

Sun R, Liu Y, Zhang H, Manuelidis L. 2008. Quantitative recovery of scrapie agent with minimal protein from highly infectious cultures. Viral Immunol 21:293–302.

Tuma RS, Beaudet MP, Jin X, Jones LJ, Cheung CY, Yue S, Singer VL. 1999. Characterization of SYBR gold nucleic acid gel stain: A dye optimized for use with 300 nm ultraviolet transilluminators. Anal Biochem 268:278–288.

Wang F, Wang X, Yuan CG, Ma J. 2010. Generating a prion with bacterially expressed recombinant prion protein. Science 327:1132–1135.

Whitley C, Gunst K, Muller H, Funk M, Zur Hausen H, de Villiers EM. 2014. Novel replication-competent circular DNA molecules from healthy cattle serum and milk and multiple sclerosis-affected human brain tissue. Genome Announc 2.

zur Hausen H. 2015. Risk factors: What do breast and CRC cancers and MS have in common? Nat Rev Clin Oncol 12:569–570.